CHAPTER 4

Thermodynamics of Mechanosensitivity

V. S. Markin* **and F. Sachs**†

*Department of Anesthesiology and Pain Management, UT Southwestern, Dallas, Texas 75235
†Physiology and Biophysical Sciences, SUNY Buffalo, New York 14214

I. OVERVIEW

Mechanosensitivity of ion channels is conventionally interpreted as being driven by a change of their in-plane cross-sectional area A_{MSC}. This, however, does not include factors relating to membrane stiffness, thickness, spontaneous curvature or changes in channel shape, length or stiffness. Because the open probability of a channel may be sensitive to multiple factors, we constructed a general thermodynamic formalism. These equations allow the

Current Topics in Membranes, Volume 58
1063-5823/07 $35.00

DOI: 10.1016/S1063-5823(06)58004-4

analysis of mechanosensitive (MS) channels in lipids of different geometric and chemical properties including hydrophobic mismatch at the boundary between the protein and lipid and the effect of changes in the bilayer intrinsic curvature caused by the adsorption of amphipaths. The model predicts that the midpoint $\gamma_{1/2}$ and the $\text{slope}_{1/2}$ of the gating curve are generally not independent, and on the basis of this relationship, we predicted the line tension at the channel/lipid border of MscL to be on the order of 10 pN suggesting that MscL channel is well matched to its lipid environment. For gramicidin, the theory predicts conversion from a stretch-activated to a stretch-inactivated gating as a function of bilayer thickness and composition.

II. INTRODUCTION

Mechanosensitivity manifests itself in many physiological processes, and MS ion channels are prototype transducers that appear to be found in all species (Bass *et al.*, 2002). As opposed to the prototypical family of homologous S4 voltage-sensitive channels, these channels are a phenotypic family with no significant homology in sequence or structure, even for channels within *Escherichia coli* (Kloda and Martinac, 2001; Martinac, 2001; Bass *et al.*, 2002; Perozo and Rees, 2003). Structural details and gating mechanisms proposed for these channels are extensively discussed in the literature (Hamill and Martinac, 2001; Betanzos *et al.*, 2002; Anishkin and Sukharev, 2004; Chiang *et al.*, 2004; Iscla *et al.*, 2004; Sukharev and Anishkin, 2004), but here we concentrate on the general principles underlying mechanical transduction by ion channels (Markin and Sachs, 2004). There appear to be two general types of MS channels: those that receive stress from fibrillar proteins and those that receive stress from the lipid bilayer. The former are associated with the specialized receptors such as cochlear hair cells (Hackney and Furness, 1995), and touch receptors in *Cenorhabditis elegans* (Garcia-Anoveros and Corey, 1996) and *Drosophila* (Walker, 2000). The channels stimulated by bilayer stress seem to be universally distributed (Sachs and Morris, 1998), although their physiological function is not generally known and do not seem to require an intact intra- or extracellular matrix in order to function (Hase *et al.*, 1995; Suchyna and Sachs, 2004). It is this latter class of channels that we address in this chapter, although the approach can be generalized to include the specific receptor families. Mechanosensitivity probably appears in all membrane channels (Gu *et al.*, 2001; Calabrese *et al.*, 2002; Laitko and Morris, 2004; Morris, 2004) and transporters (Jutabha *et al.*, 2003; Gradmann and Boyd, 2005) in the same way as their activity is modulated by membrane potential.

The bacterial channels have nanosiemens conductances that do not significantly distinguish anions from cations, and are phenotypically and structurally

different from the channels in eukaryotes such as the 2P (Patel *et al.*, 2001; Honore and Patel, 2004) and TRP (Kim, 2004; Lin *et al.*, 2005; Maroto *et al.*, 2005) channels. The requirements for channels to become MS appear not to require specialized local structures such as utilized by the S4 voltage-sensitive channel family but have probably evolved many times. Mechanosensitivity simply requires a significant change in channel dimensions between the closed and open states. The relevant stresses are global such as the far-field tension and intrinsic curvature, or local such as amphipath modulation of boundary lipids (Martinac *et al.*, 1990; Markin and Martinac, 1991; Hwang *et al.*, 2003). These stresses interact with the changes in channel dimensions to change the relative energy of the closed and open states.

There are three basic types of channel deformation that can change energies of the states (Fig. 1): change of in-plane area, change of shape, or change of length normal to the membrane. If a channel increases its in-plane

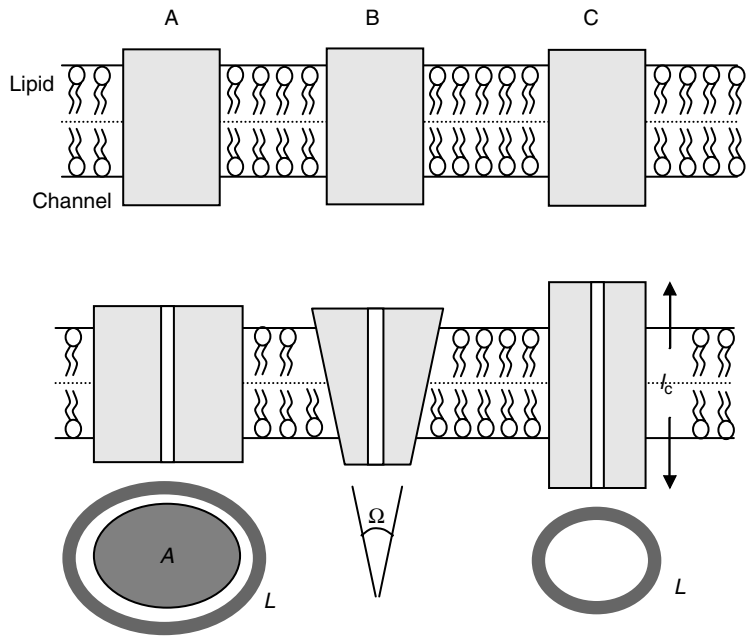

FIGURE 1 Cartoon of three basic types of MS channel deformation during transition between closed and open states. (A) A change of area A occupied by the channel in plane of the membrane also changes the length L of the border between the channel complex and surrounding lipid where the line tension f resides; the "shape" of the complex does not change. (B) A change of shape of the MS expressed as a body angle Ω; average in-plane area of the complex does not change. (C) Change of the length l_c of the MS complex normal to the membrane; it can lead to changes in line tension f at the border with lipid.

area A (case A) (Sachs and Lecar, 1991), the channel is stretch-activated (SAC). If the area decreases, it is stretch-inactivated (SIC) (Morris and Sigurdson, 1989).

In another limiting case, an MS channel can change its shape, expressed as a body angle Ω, without changing its in-plane area (case B). This type of mechanosensitivity is called shape sensitivity (Petrov and Usherwood, 1994; Petrov, 1999). The movement can be assisted (or resisted) by torque M produced by membrane curvature. The torque in the membrane can be produced either by global bending or by introduction of noncylindrical lipids such as lysolipids.

The third limiting case of deformation (case C) is a change of the length l_c of the channel without a change of in-plane area or shape. This can result in hydrophobic mismatch between an MS channel and the surrounding lipid bilayer and is expressed as a line tension along the border with lipid. If the bilayer is stretched, or thinned with voltage, then its thickness decreases, changing the hydrophobic mismatch for open and closed states. If the energy of the closed state increases relative to the energy of open state, then the channel will tend to open under tension. This type of mechanosensitivity is called the length sensitivity. Natural MS channels may combine one or more of these basic deformations.

A. General Equations

Deformation of the channel is described by the Gibbs free energy that consists of three contributions: MS channel area, shape, and length

$$\begin{aligned} G_A &= U_0 + \frac{1}{2}B(A_{MSC} - A_0)^2 + fL - \gamma A_{MSC} \\ G_\Omega &= -M\Omega \\ G_l &= fL \end{aligned} \tag{1}$$

Here B is the area stiffness (sometimes denoted K_A), and A_0 is the in-plane area of the closed channel, and A_{MSC} the in-plane area of the open channel, f is the line tension at the border between the MS channel and surrounding lipids, L is the length of this border (Fig. 1). The shape of the MS channel can be described by the body angle Ω which changes in the transition and can be influenced by the total torque M acting on the MS channel.

The area Gibbs energy G_A describes the phenomenon of mechanosensitivity per se because it is directly related to membrane stretching. The body angle Gibbs energy G_Ω is not necessarily related to membrane stretching and may occur without it. It describes ion channels that are not MS in conventional sense, but do respond to local mechanical stresses. Changing the

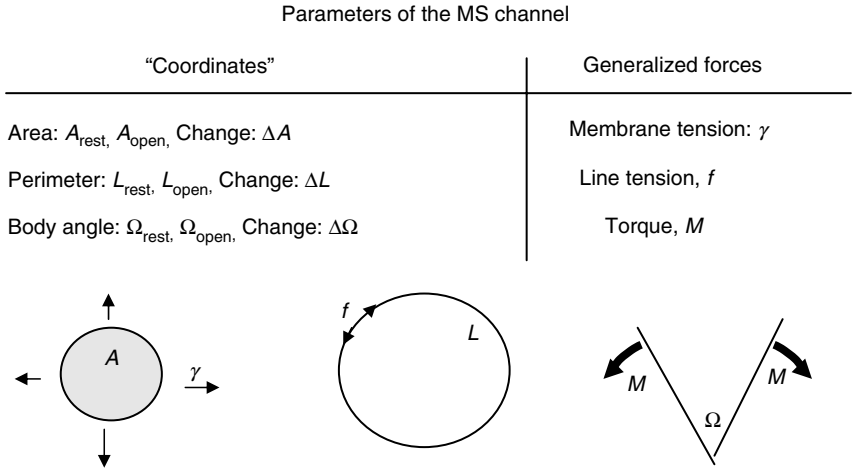

FIGURE 2 Parameters of MS channels. The cartoon presents generalized coordinates (area, perimeter, and body angle) and generalized forces (membrane tension, line tension, and torque).

composition of the membrane can also alter gating of the channels. Therefore, there are three pairs of generalized coordinates and forces (Fig. 2): area–membrane tension, perimeter–line tension, and body angle–torque.

III. AREA SENSITIVITY

In the absence of line tension, the gating of an MS channel is described as the transition between two energy levels corresponding to the closed and open states,

$$\begin{aligned} G_{\mathrm{A}}^{\mathrm{close}} &= U_0^{\mathrm{close}} + \frac{1}{2} B^{\mathrm{close}} (A_{\mathrm{MSC}} - A_0^{\mathrm{close}})^2 - \gamma A_{\mathrm{MSC}}, \\ G_{\mathrm{A}}^{\mathrm{open}} &= U_0^{\mathrm{open}} + \frac{1}{2} B^{\mathrm{open}} (A_{\mathrm{MSC}} - A_0^{\mathrm{open}})^2 - \gamma A_{\mathrm{MSC}} \end{aligned} \tag{2}$$

Transitions occur between the two minima of these curves. Let us consider the case when the elasticity moduli of both states are equal to B (Fig. 3). In the closed state, the coordinates of the minimum of the energy curve are given by $A_{\mathrm{min}}^{\mathrm{close}} = (\gamma/B) + A_0^{\mathrm{close}}$ and $G_{\mathrm{A,min}}^{\mathrm{close}} = U_0^{\mathrm{close}} - (\gamma^2/2B) - \gamma A_0^{\mathrm{close}}$. The same coordinates for the open state are $A_{\mathrm{min}}^{\mathrm{open}} = (\gamma/B) + A_0^{\mathrm{open}}$ and $G_{\mathrm{A,min}}^{\mathrm{open}} = U_0^{\mathrm{open}} - (\gamma^2/2B) - \gamma A_0^{\mathrm{open}}$. Therefore, in the transition from closed to open, the area changes by,

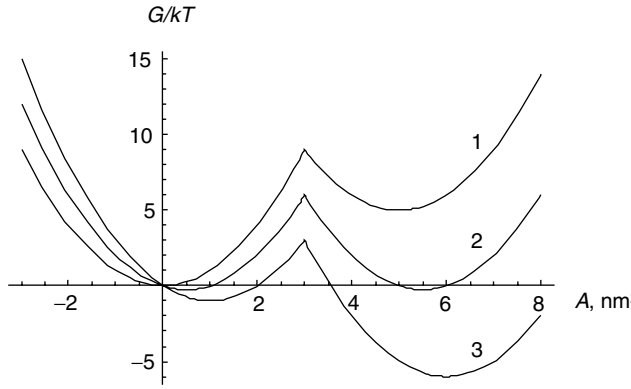

FIGURE 3 Plot of energy of the MS channel in closed (left part) and open (right part) states. Curve 1 is plotted in the absence of membrane tension, curve 2 corresponds to the midpoint of the transition, and curve 3 corresponds to the completely open state.

$$\Delta A_{\min} = A_{\min}^{\text{open}} - A_{\min}^{\text{close}} = A_0^{\text{open}} - A_0^{\text{close}} \equiv \Delta A_0 \tag{3}$$

and the energy by,

$$\Delta G_{\text{A,min}} = G_{\text{A,min}}^{\text{open}} - G_{\text{A,min}}^{\text{close}} = \Delta U_0 - \gamma \Delta A_0 \tag{4}$$

These equations and Fig. 3 show that with increasing tension, the minimum shifts down and to the right. Notice that the distance between the minima on the area axis ΔA does not change, while on the energy axis it decreases, becomes zero, and then again increases in another direction.

The open probability of the channel is defined by the Boltzmann function,

$$p_{\text{open}} = \frac{1}{1 + \exp(\Delta G_{\min}/kT)} \tag{5}$$

and hence it increases with γ as shown in Fig. 4, changing from 0 to 1. The curves in Fig. 3 represent three characteristic states. Curve 1 is drawn in the absence of membrane tension, $\gamma = 0$. The energy difference between the two minima is large, and the channel is closed. On the Boltzmann curve (Fig. 4), this point is shifted far to the left. Curve 2 represents the situation when the two minima are at the same level, $\Delta G_{\min} = 0$, and hence $p_{\text{open}} = 1/2$. The corresponding membrane tension is designated $\gamma_{1/2}$. Curve 3 corresponds to high tension and is associated with the open channel. There are two parameters characterizing this function $p_{\text{open}}(\gamma)$: the midpoint of the transition $\gamma_{1/2}$ and the slope of the curve at this point (the slope sensitivity) equal to $\Delta A_0/4kT$.

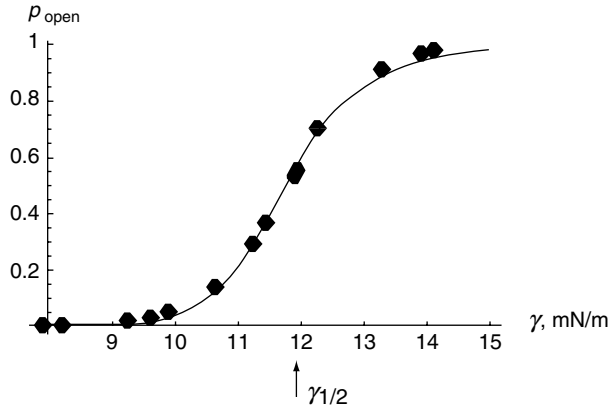

FIGURE 4 Open probability as a function of membrane tension.

The two-state model with equal rigidity described the kinetics of MscL but runs into difficulties (Sukharev and Markin, 2001). The parameter of mechanosensitivity, ΔA_0 at the midpoint of the transition, was found to be $\sim$6 nm^2. However, the X-ray structure of the channel predicted that the difference of in-plane area between the open and closed states should be about 20 nm^2! This huge discrepancy has to be explained, and there are a few ways to do this. One is to assume different elasticity moduli in the closed and open states. Sukharev and Markin (2001) assumed that $B_{closed} < B_{open}$. Then the transition parameter ΔA is no longer independent of membrane tension:

$$\Delta A_{min} = A_{min}^{open} = \frac{\gamma}{B} + A_0^{open} = \Delta A_0 - \left(\frac{1}{B^{close}} - \frac{1}{B^{open}}\right)\gamma \qquad (6)$$

Figure 5 illustrates this situation. With increasing γ, the transition parameter ΔA_{min} decreases. If in the beginning it was equal to 18.5 nm^2, then at the middle point of transition it is about 6 nm^2. We have to add that this explanation still utilizes the simple two-state model, though more sophisticated alternatives were suggested (Sukharev and Anishkin, 2004).

A. Line Tension and Area Sensitivity

The area Gibbs free energy as a function of A_{MSC} has a minimum at the point determined by the equation,

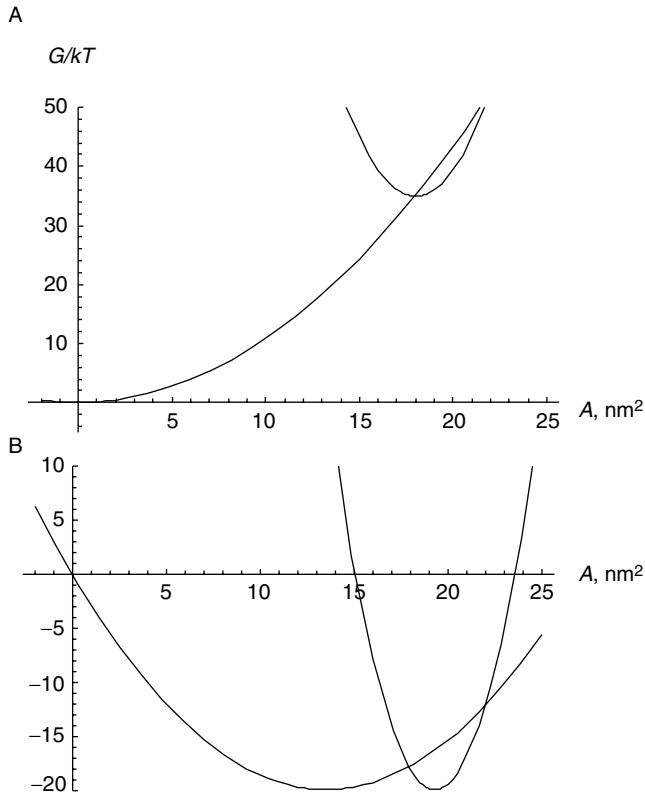

FIGURE 5 Energy plots of MS channel with different elasticity in closed and open states. (A) No membrane tension; (B) midpoint of transition.

$$B(A_{\min} - A_0) + \frac{f}{\sqrt{\pi A_{\min}}} - \gamma = 0 \tag{7}$$

If the energy associated with the line tension is small compared to that associated with change in area, then:

$$A_{\min} \approx \frac{\gamma}{B} + A_0 - \frac{f}{\sqrt{\pi} B \sqrt{\frac{\gamma}{B} + A_0}} \tag{8}$$

Notice that $A_{\min}$ decreases with line tension f, as to be expected from compression of the channel at its periphery. The minimal value of G is given by,

$$G_{\min} = U_0 - \gamma A_0 - \frac{\gamma^2}{2B} + \frac{2f}{\sqrt{\pi}}\sqrt{\frac{\gamma}{B} + A_0} \tag{9}$$

and the difference between two minima is:

$$\Delta G_{\min} = \Delta U_0 - \gamma \Delta A_0 - \frac{\gamma^2}{2}\left(\frac{1}{B_{\text{open}}} - \frac{1}{B_{\text{close}}}\right) + \frac{2f}{\sqrt{\pi}}\left(\sqrt{\frac{\gamma}{B_{\text{open}}} + A_0^{\text{open}}} - \sqrt{\frac{\gamma}{B_{\text{close}}} + A_0^{\text{close}}}\right) \tag{10}$$

Now, the open probability of the channel defined by the Boltzmann function is,

$$p_{\text{open}} = \frac{1}{1 + \exp(\Delta G_{\min}/kT)} \tag{11}$$

To further simplify the calculations, let us assume that the stiffness of the closed and open states are equal, that is, the Young's moduli B_{open} and B_{close} are equal to B (but see Sukharev *et al.*, 1999). Then the midpoint of the transition, when $p_{\text{open}} = 1/2$, is:

$$\gamma_{1/2} = \frac{\Delta U_0}{\Delta A_0} + \frac{2f}{\sqrt{\pi}\,\Delta A_0}\left(\sqrt{\frac{\Delta U_0}{B\Delta A_0} + A_0^{\text{open}}} - \sqrt{\frac{\Delta U_0}{B\Delta A_0} + A_0^{\text{close}}}\right) \tag{12}$$

The slope of the curve at the midpoint is:

$$S = \text{Slope}_{1/2} = \frac{\mathrm{d}p_0}{\mathrm{d}\gamma} = \frac{1}{4kT}\left[\Delta A_0 + \frac{\gamma_{1/2}\Delta A_0 - \Delta U_0}{B\sqrt{(\Delta U_0/B\Delta A_0) + A_0^{\text{open}}}\sqrt{(\Delta U_0/B\Delta A_0) + A_0^{\text{close}}}}\right] \tag{13}$$

Notice that both the position of the midpoint (12) and the slope of the curve (13) depend on the line tension, and they both increase with increasing f.

These equations contain a few characteristic parameters. The first equation can be transformed to,

$$\gamma_{1/2} = \frac{\Delta U_0}{\Delta A_0} + \frac{2f}{\sqrt{\pi}\left(\sqrt{(\Delta U_0/B\Delta A_0) + A_0^{\text{open}}} + \sqrt{(\Delta U_0/B\Delta A_0) + A_0^{\text{close}}}\right)} \tag{14}$$

The first term in this sum gives the characteristic membrane tension when the line tension f is zero:

$$\gamma_0 = \frac{\Delta U_0}{\Delta A_0} \tag{15}$$

By the analysis of the dimensions, one can establish that the denominator in the second term represents a characteristic length λ,

$$\lambda = \frac{\sqrt{\pi}}{2}\left(\sqrt{(\Delta U_0/B\Delta A_0) + A_0^{\text{open}}} + \sqrt{(\Delta U_0/B\Delta A_0) + A_0^{\text{close}}}\right), \tag{16}$$

which converts line tension f to membrane tension γ. The physical meaning of this parameter is as follows. The ratio f/λ gives the force compressing the MS channel. Therefore to open the channel, the membrane tension should be increased by this amount, and λ is the *effective* radius of a cylinder surrounding the channel, not necessarily a van der Waals enclosure.

Finally, the tension at the midpoint of the transition can be presented as,

$$\gamma_{1/2} = \gamma_0 + \frac{f}{\lambda} \tag{17}$$

Analogously the slope of transition at the midpoint can be transformed to,

$$S = \frac{\Delta A_0}{4kT}\left[1 + \frac{f}{\lambda\gamma_s}\right], \tag{18}$$

where the denominator contains a characteristic membrane tension,

$$\gamma_s = \sqrt{\left(\frac{\Delta U_0}{\Delta A_0} + A_0^{\text{open}}B\right)\left(\frac{\Delta U_0}{\Delta A_0} + A_0^{\text{close}}B\right)} \tag{19}$$

Comparing two characteristic tensions (15) and (19), one can see that

$$\gamma_s > \gamma_0 \tag{20}$$

These equations describe the role of line tension in the apparent area sensitivity.

B. *Direct Observations of the Effect of Line Tension and Shape Transformation*

MS channels can be reconstituted in different lipid bilayers (Perozo *et al.*, 2002; Moe and Blount, 2005) permitting the evaluation of local physical mechanisms for a role in MS channel gating: the hydrophobic mismatch at

the boundary between the protein and lipid and variations of bilayer intrinsic curvature. In addition, control of lipid composition permits altering f with heard group variation (Moe and Blount, 2005). The first mechanism can be attributed to the variation of the line tension around the molecule (area variation), and the second can be described by the body angle variation. Perozo *et al.* (2002) studied the bacterial wild-type MscL in DPPC bilayers with monosaturated chains of 16, 18, and 20 carbons. They found that the midpoint of the gating transition and the slope of the transition in all three bilayers were different. With increasing lipid chain length, there was a parallel increase of both the midpoint and the slope of the transition (Fig. 6), which is in correspondence with theoretical predictions from Eqs. (17) and (18) if we assume that the line tension increases with lipid thickness.

The detailed analysis of the intrinsic parameters of the channel and their variation from one membrane to another was done in Markin and Sachs (2004). They used the normalized values of midpoint membrane tension $r_t = \gamma_{1/2}/\gamma_{1/2}(16)$ and the slope of transition $r_s = s/s(16)$. Using Eq. (17), the first ratio of two tensions was presented as

$$r_t = \frac{\gamma_{1/2}(n)}{\gamma_{1/2}(16)} = \frac{1 + [f(n)/\lambda\gamma_0]}{1 + [f(16)/\lambda\gamma_0]} = \frac{1 + g(n)}{1 + g(16)} \tag{21}$$

And the function $g(n)$ was found as:

$$g(n) = -1 + 0.5714(0.0625n^2 - 1.75n + 13) \tag{22}$$

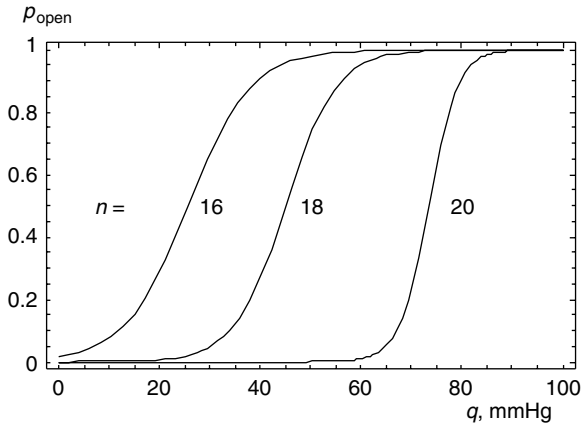

FIGURE 6 Open probability p_{open} of MS channel as a function of the trans-patch hydrostatic pressure q. Numbers on the curves indicate the length of the lipid chain.

The experimental points are presented in Fig. 7A. To find the line tension at different points, one needs to estimate the characteristic length λ. Equation (16) can be simplified to:

$$\lambda \approx \frac{\sqrt{\pi}}{2}\left(\sqrt{A_0^{\text{open}}} + \sqrt{A_0^{\text{close}}}\right) \tag{23}$$

If the cross section of the molecule were circular, then λ could be expressed via the radii of the molecules in open and closed states: $\lambda = \pi(r_0^{\text{open}} + r_0^{\text{close}})/2$ and is proportional to the average radius of the MS channel in the transition state.

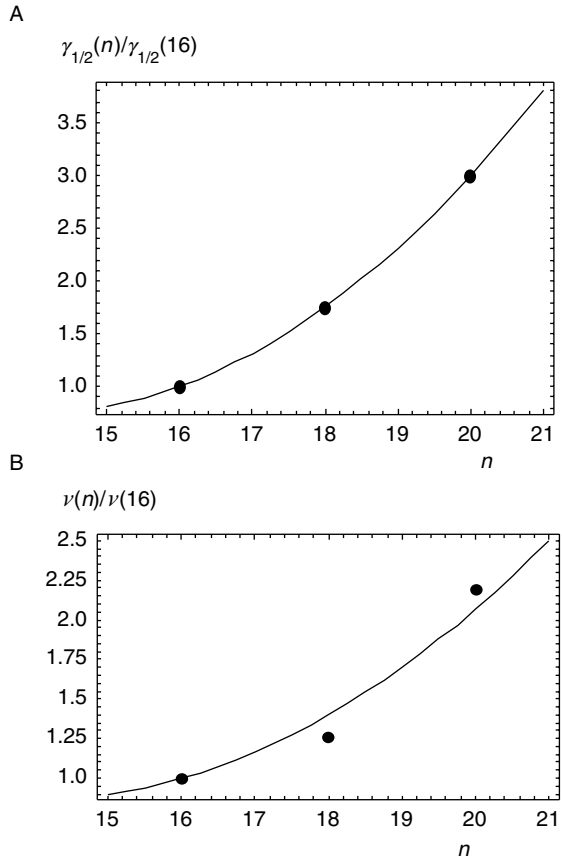

FIGURE 7 Parameters of the MS channel as the functions of the length of the lipid chain. (A) Membrane tension corresponding to the midpoint of the transition. (B) Slope of the transition curve at the midpoint.

Parameter was $\lambda \sim 8.8$ nm, and the predicted line tension was $f(18) \sim 10.6$ pN, and $f(20) \sim 25.6$ pN. For comparison, the line tension of the hydrophobic edge of a phospholipid membrane against water is 120 pN, so the mismatch of the lipid at the MS molecule comprises only a fraction of the potential hydrophobic edge energy.

The function $f(n)$ also predicts the slope of the transition (Fig. 7B). The ratio of the slopes is given by:

$$r_s = \frac{1 + [f(n)/\lambda\gamma_s]}{1 + [f(16)/\lambda\gamma_s]} = \frac{1 + g(n)/\xi}{1 + g(16)/\xi} \tag{24}$$

with $\xi = 1.5$ and characteristic tension of $\gamma_s = 2.4$ mN/m. In accordance with the theory, this value exceeds the resting tension $\gamma_0 = 1.6$ mN/m.

IV. SHAPE SENSITIVITY

If the channel complex is shape sensitive, then its open probability will be affected by torque M in the membrane: $p_{\text{open}} = \text{function}(M)$. The torque is related to membrane curvature that can be affected by applied pressure (Sokabe *et al.*, 1991; Akinlaja and Sachs, 1998), for example, and intrinsic curvature. In particular, it can be generated by different concentrations, c_{out} and c_{in}, of conical molecules in the two membrane leaflets (Fig. 8):

$$M = \alpha(c_{\text{out}} - c_{\text{in}}) \tag{25}$$

If the shape of the molecule can be described by a single parameter—a certain body angle Ω, then its shape deformation energy can be presented in the same way as for area sensitivity:

$$G_\Omega = U_0 + \frac{1}{2}K_\Omega(\Omega - \Omega_0)^2 - M\Omega, \tag{26}$$

where K_Ω is the shape elasticity modulus. The energy of transition can be given by,

$$\Delta G_{\Omega,\min} = \Delta U_0 - M\Delta\Omega_0 \tag{27}$$

The open probability, as before, is given by Eq. (11), which transforms to:

$$p_{\text{open}} = \frac{1}{1 + \exp\{[a + b(c_{\text{out}} - c_{\text{in}})]/kT\}} \tag{28}$$

This is the simplest case when the shape can be effectively described by a single parameter—body angle. This kind of channel is activated when the molecule is deformed in one direction and inactivated in another (Fig. 9A).

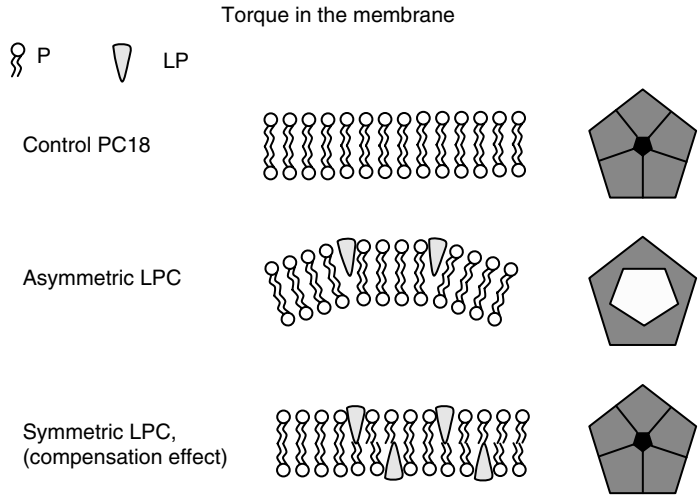

FIGURE 8 Torque in the membrane. Torque is created by an asymmetric distribution of LPC in two membrane leaflets. Appearance of lysolipids creates torque even if the global curvature does not change. In other words, the effect can be described as change of spontaneous curvature.

This is called one-sided shape activation, and this phenomenon has been observed *in vitro* (Bowman and Lohr, 1996b).

One can imagine another mechanism: the channel opens when the body angle is deformed in the both positive and negative directions (Fig. 9B). It is two-sided shape activation, and the open probability in the first approximation can be presented as,

$$p_{\text{open}} = \frac{1}{1 + \exp\{[a + b(c_{\text{out}} - c_{\text{in}})^2]/kT\}} \tag{29}$$

A. Experimental Observation of Shape Sensitivity

It was reported in a number of papers that addition of charged amphiphiles, or lysophospholipids (LPL), to bilayers containing MS channels, dramatically lowered the activation threshold. With MscL, externally applied lysophosphatidylcholine (LPC) strongly favors the open state. The addition of LPC (1.5 μM), in the presence of a small transbilayer pressure, produces a pronounced increase in MscL activity. Moreover, once the pressure is released, a large fraction of the channels remain constitutively open. Even more

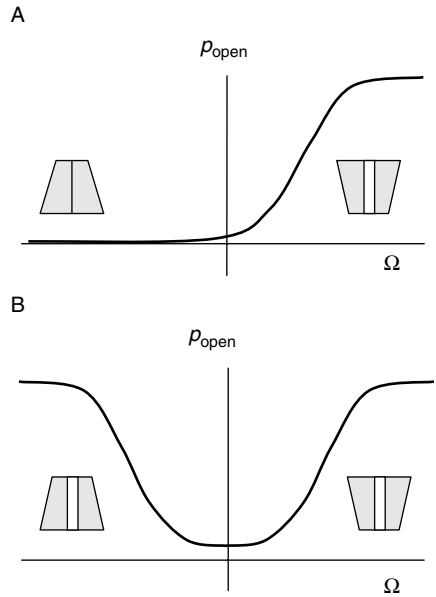

FIGURE 9 Shape sensitivity of the MS channel. The MS molecule deforms in the positive direction ($\Omega > 0$ or upper side is larger than lower side) and/or the negative direction ($\Omega < 0$ or upper side is smaller than lower side). If the channel can open only when deformed in the positive direction, this is one-sided shape sensitivity (panel A). Another possibility is that it opens in both directions; this is two-sided shape sensitivity (panel B).

remarkably, at larger LPC concentrations (3 μM), MscL activity gradually increased with time in the absence of any applied pressure. It is important to remember, however, that there is always a resting tension present due to the energy of adhesion of the lipid for the glass (Opsahl and Webb, 1994).

The LPC effects suggest a second type of mechanosensitivity. The asymmetric addition of conically shaped LPC in the outer monolayer generates the torque that affects the transition of MscL. At the same time it suggests that the gating of MscL is accompanied by a shape change. Remarkably, Perozo *et al.* (2002) found that if LPC is added symmetrically to both monolayers, the gating does not change. This is explained by the fact that LPC in two different leaflets produces opposite effect because $m_{in} = -m_{out}$ and hence $M = 0$, and there is no effect on the energy of the channel. Given that MscL is not symmetric along the membrane normal, the effects of LPC may be asymmetric also. However, preliminary data suggest that if

LPC was added to the inner monolayer only, the channel would also be activated (B. Martinac, private communication). If true, that would make the channel belong to the two-sided shape activation family.

An example of one-sided shape activation channel was found by Maingret *et al.* (1999, 2000). They studied the MS K^+ channels TREK-1 and TRAAK, and found that they too can be activated by LPLs and other amphipaths. LPC activation was a function of the size of the polar headgroup, and length of the acyl chain, but independent of the charge. These channels, which are found commonly in the central nervous system, are also opened by inhalation anesthetics such as chloroform, ether, halothane, and isoflurane at clinically relevant concentration (Patel *et al.*, 1999). The authors proposed that activation of these K^+ channels may form the basis of general anesthesia. Perhaps MS channels evolved as amphipath detectors (Patel *et al.*, 2001), and only later the far-field mechanosensitivity became useful.

While amphipaths can cause changes in global membrane curvature, that effect appears to be a correlation rather than the cause of changes in MS channel gating. Amphipaths probably act locally (Suchyna *et al.*, 2004b). We should not expect that global bilayer curvature (Sukharev *et al.*, 1999; Moe and Blount, 2005) can change channel gating. For molecular sized objects like channels, the available energy input from changes in global curvature (radius of curvature > 1 μm) is well below kT_B, and thus cannot have a significant effect on gating. Indeed, if the in-plane area of the MS molecule is A, bending rigidity is K_B and the radius of curvature is R_p, then its bending energy is $E_{bend} = \frac{1}{2} K_B (2/R_p)^2 A$. Bending rigidity of MS channel is unknown so we substitute for it the bending rigidity of the lipid bilayer. For freely sliding monolayers K_B can be estimated (Markin and Albanesi, 2002) as $0.8 \times 10^{-19} J = 20\, kT$. Taking $A = 30$ nm^2 and $R_p = 1$ μm, one can find $E_{bend} = 1.2 \times 10^{-3}\, kT$. This is indeed a small amount. Even if to vary the parameter in this equation in reasonable range, one cannot approach $1\, kT$!

There is no data to suggest that MS channels are, in fact, sensitive to global bilayer curvature (Lee, 2006), but there is evidence for membrane curvature sensitivity in biological membranes. The 2P K^+ channels, and some cationic MS channels, demonstrate pronounced curvature sensitivity, activating with curvature away from the cell (Maingret *et al.*, 2000, 2002) or toward the cell (Bowman and Lohr, 1996a). Even the breaking strength of biological membranes is sensitive to the sign of the curvature, being stronger when bent toward the cytoplasm (Akinlaja and Sachs, 1998). This curvature sensitivity reminds us to be cautious applying simple homogenous physical models to the heterogeneous and anisotropic biological membranes.

V. LENGTH SENSITIVITY AND SWITCH BETWEEN STRETCH-ACTIVATION AND STRETCH-INACTIVATION MODES

Gramicidin is a wonderful example of a channel that does not change either in-plane area or shape. From a conventional point of view, it should not be MS. Nevertheless, it can be activated by either membrane stretch or membrane torque. In addition, it can switch between activation and inactivation modes (Hamill and Martinac, 2001; Martinac and Hamill, 2002). As an example of the utility of the general thermodynamic approach, we will analyze gramicidin.

Gramicidin A (gA) forms dimer channels, with the gA in one monolayer binding to a mate in the opposite monolayer (Andersen *et al.*, 1996) (Fig. 10). Other than head–head dimer formation, gA does not change its conformation significantly between open and closed, and still it is strongly influenced by mechanical stresses in the bilayer. The allosteric parameter governing activation and inactivation is membrane thickness.

The process of channel formation is described by the dimerization reaction between two monomers (m) from adjacent lipid leaflets (Lundbaek and Andersen, 1994). If the numbers of monomers in two leaflets are equal (N_m) and the number of dimers is N_d then in equilibrium,

$$\begin{aligned} k_{+1}N_m^2 - k_{-1}N_d &= 0 \\ N_m + N_d &= N_{tot} \end{aligned} \tag{30}$$

where N_{tot} is total amount of gramicidin in each leaflet and k_{+1} and k_{-1} are the reaction rates. Solution of these equations is

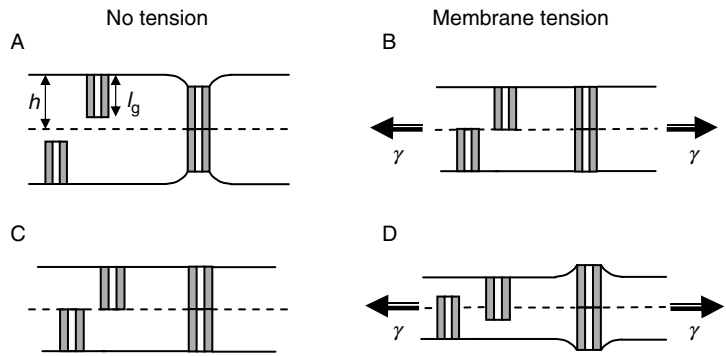

FIGURE 10 Gramicidin A in the lipid bilayer: formation of dimers causes deformation of the bilayer.

$$N_{\mathrm{d}} = \frac{2K_{\mathrm{D}}N_{\mathrm{tot}} + 1 - \sqrt{4K_{\mathrm{D}}N + 1}}{2K_{\mathrm{D}}}, \tag{31}$$

where $K_{\mathrm{D}} = k_{+1}/k_{-1}$ is the dimerization constant. If $K_{\mathrm{D}}N_{\mathrm{tot}} \ll 1$, which is usually the case, then $N_{\mathrm{d}} \approx K_{\mathrm{D}}N_{\mathrm{tot}}^2$. The dimerization constant includes the free Gibbs energy of transition:

$$K_{\mathrm{D}} = K_* \exp\left(-\frac{\Delta G}{kT}\right), \tag{32}$$

where K_* is the pre-exponential coefficient not depending on temperature.

The free Gibbs energy of transition can be found in the following way. If the length of the dimer does not coincide with the thickness of the hydrophobic core of the bilayer (Fig. 10A and D), then the hydrophobic mismatch with a formed channel will cause deformation of the bilayer with positive or negative local curvature (Hladky and Haydon, 1972). As demonstrated above, this deformation is equivalent to a line tension around the dimer, changing its energy relative to the two monomers. So the Gibbs free energy difference between these two states can be presented as

$$\Delta G = fL - G_{\mathrm{ass}}, \tag{33}$$

where L is the length of the perimeter and G_{ass} is the component of the energy of association that does not depend on membrane thickness. The degree of the deformation of the membrane depends on the relationship between the thickness of the monolayer h and the length of gramicidin l_{g}. Their difference $m = l_{\mathrm{g}} - h$ determines the value of the deformation energy and hence the line tension; in the Hookean approximation it can be presented as

$$f = k_{\mathrm{m}}(h - l_{\mathrm{g}})^2, \tag{34}$$

where k_{m} is the proportionality coefficient. The applicability of the Hookean approximation to this case was discussed by Lundbaek and Andersen (1999) and Lundbaek *et al.* (1997) who demonstrated that the deformation energy can be quantified based on a linear spring description. When membrane tension γ is applied, the membrane area A_{m} increases. Due to the volume incompressibility of lipids (Ah = constant), the thickness of monolayers h decreases:

$$\frac{\Delta h}{h_0} = -\frac{\Delta A_{\mathrm{m}}}{A_{\mathrm{m}}} = -\frac{\gamma}{K_{\mathrm{A}}} \tag{35}$$

where h_0 is the monolayer thickness in the absence of membrane tension, and K_{A} is the elasticity modulus of the lipid bilayer. Then the line tension is

$$f = k_{\mathrm{m}}\left(h_0 - l_{\mathrm{g}} - h_0\frac{\gamma}{K_{\mathrm{A}}}\right)^2 \tag{36}$$

and the Gibbs energy can be presented as:

$$\Delta G = Lk_{\mathrm{m}}h_0^2\left(1 - \frac{l_{\mathrm{g}}}{h_0} - \frac{\gamma}{K_{\mathrm{A}}}\right)^2 - G_{\mathrm{ass}} \tag{37}$$

where L is the external perimeter of gramicidin. The number of dimers is

$$N_{\mathrm{d}} = K_* N_{\mathrm{tot}}^2 \exp\left(-\frac{\Delta G}{kT}\right) = K_* N_{\mathrm{tot}}^2 \exp\left(\frac{G_{\mathrm{ass}}}{kT}\right)\exp\left[-\frac{Lk_{\mathrm{m}}h_0^2}{kT}\left(1 - \frac{l_{\mathrm{g}}}{h_0} - \frac{\gamma}{K_{\mathrm{A}}}\right)^2\right] \tag{38}$$

One can introduce the maximum number of dimers that can be formed by membrane stretching $N_{\mathrm{d}}^{\max} = K_* N_{\mathrm{tot}}^2 \exp(G_{\mathrm{ass}}/kT)$ and can define the ratio $p_{\mathrm{open}} = N_{\mathrm{d}}/N_{\mathrm{d}}^{\max}$ as the open probability:

$$p_{\mathrm{open}} = \exp\left[-\frac{Lk_{\mathrm{m}}h_0^2}{kT}\left(1 - \frac{l_{\mathrm{g}}}{h_0} - \frac{\gamma}{K_{\mathrm{A}}}\right)^2\right] \tag{39}$$

The definition of this parameter as an open probability is not very rigorous because the channels do not exist *a priori*, but rather are formed in the process of stretching. It might be better to call it the degree of activation. Nevertheless, we shall use this definition in this section, because the number of open channels cannot exceed $N_{\mathrm{d}}^{\max}$. However, in the next section this parameter will be discussed in more details.

The degree of activation or the open probability (39) is a function of two variables: $p_{\mathrm{open}} = p_{\mathrm{open}}(h_0, \gamma)$ (Goulian *et al.*, 1997). With increasing membrane tension, the p_{open} can decrease or increase, depending on the thickness of the monolayer, h_0. The phase space $[h_0, \gamma]$ presented in Fig. 11 is divided into two parts corresponding either to stretch-inactivation of the channels, or stretch-activation. Interestingly enough, if $h_0 \leq l_{\mathrm{g}}$ then application of membrane tension causes inactivation of the channels. However, if $h_0 > l_{\mathrm{g}}$ the behavior is more complicated. Small tensions cause activation of the channels, but after exceeding some critical value corresponding to a point at the curve in Fig. 11, the channels become SIC. Open probability, corresponding to these two cases is presented in Fig. 12A. The general case is presented in three-dimensional plot in Fig. 12B.

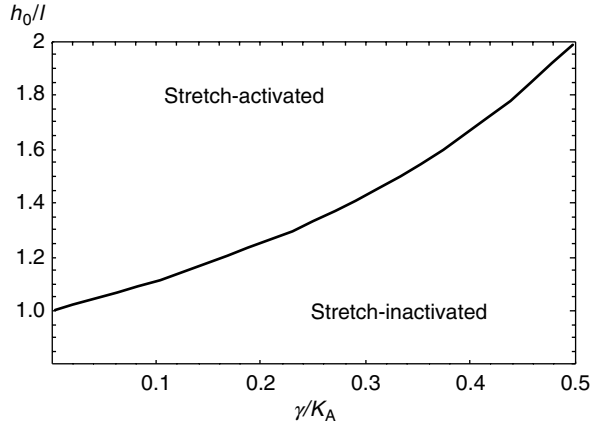

FIGURE 11 Phase space $[h_0, \gamma]$ is divided into two parts corresponding either to stretch-inactivation of the channels or to stretch-activation. The curve gives the maximum of the open probability presented by Eq. (39).

If membrane tension can influence formation of dimers, then there should be a force normal to the membrane that pulls the monomers inside the bilayer or pulls them apart disrupting the channel. This force is exerted by the deformed border area of lipid monolayers as presented in Fig. 10. The value of this force F_{normal} can be found from the energy of deformation (37) and (34):

$$F_{\text{normal}} = -\frac{\mathrm{d}\Delta G}{\mathrm{d}h} = 2Lk_{\text{m}}(l_{\text{g}} - h) \equiv 2Lk_{\text{m}}\left[l_{\text{g}} - h\left(1 - \frac{\gamma}{K_{\text{m}}}\right)\right] \tag{40}$$

The sign of the force is selected in such a way that positive force ($l_{\text{g}} - h > 0$) compresses the dimers inside the bilayer, as in Fig. 10D, while negative forces (when $l_{\text{g}} - h < 0$) pull them apart, as in Fig. 10A. Both positive and negative forces prevent formation of the channels. This is obvious in the thick bilayer where this force pulls the monomers apart. But it is also true in thin bilayers, where the force pulls the monomers inside, because the energy of the dimer protruding from the membrane is higher than fitting deeper side by side. This can also be viewed as the thin membrane preventing channel formation because the interior faces of the gA cannot interact since the gA monomers bump into each other side-by-side. Global membrane tension changes these forces by changing the thickness of the monolayer h; it decreases the magnitude of the negative force in Fig. 10A and eliminates its destructive influence on channel formation. This stretch-activation situation happens in thick monolayers. In thin monolayers, we have the opposite case:

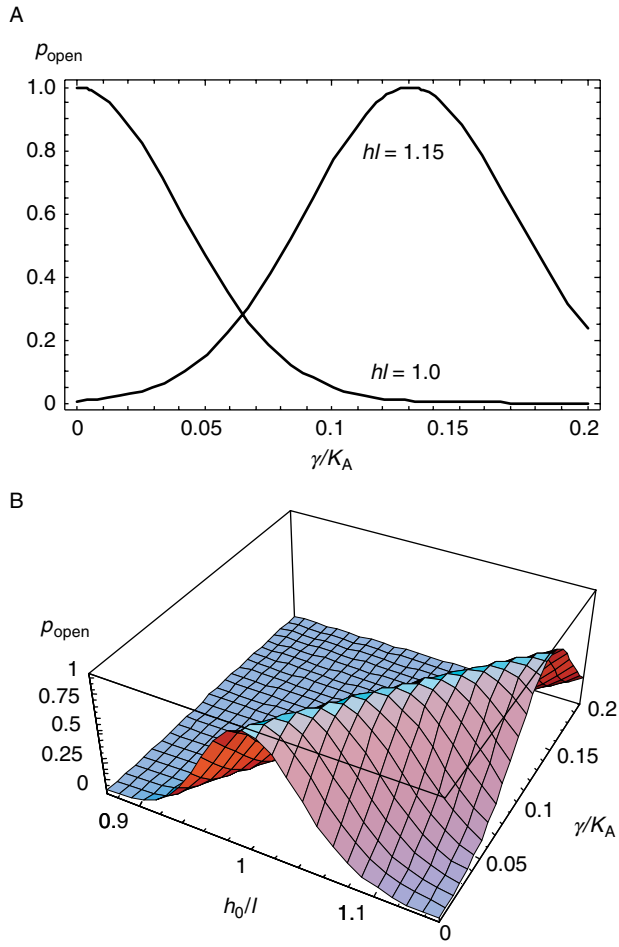

FIGURE 12 Open probability P_0 as a function of two dimensionless variables h_0/l_g and γ/K_A according to Eq. (39). For illustrative purposes, we arbitrarily selected $Lk_m h_0^2/kT = 300$. (Panel A) Two curves corresponding to $h_0/l_g = 1$ and $h_0/l_g = 1.1$. These are cross sections of the surface presented in panel B. (Panel B) Three-dimensional plot of function (39).

The force does not decrease but rather increases and prevents formation of dimers.

Therefore, the general rule is that in thin membranes, gA channels should be SIC, while in thick membranes they are stretch-activated at small tensions, but switch polarity at high tensions. This difference of polarity in thin

and thick bilayers was observed (Hamill and Martinac, 2001), but Eq. (39) predicts more than that: It says that the switch from stretch-activation to stretch-inactivation can occur in the same membrane at sufficiently large tensions. However, channel opening usually occurs at relatively high membrane tensions. Therefore, to observe the curve marked 1.15 in Fig. 12A, one might need tensions greater than the lytic limit (~10 mN/m). However, the lytic strength of membranes depends on duration of the stimulus, so that short duration stimuli can apply much higher tensions without lysis (Evans *et al*., 2003). We leave this prediction for the experimentalists.

A. Channel Activation by LPLs

Another interesting question is the role of membrane torque generated by LPLs. We demonstrated above that if the channel changes shape during the transition between two states, then the addition of LPLs can either facilitate or inhibit this transition. Gramicidin channel does not change shape so that torque should not have direct effect. However, if there is a hydrophobic mismatch as in Fig. 12A, then the monolayer bends with a positive curvature. If LPLs are added, they can generate a positive torque, and facilitate monolayer bending in the same direction. They should facilitate stretch-activation of the gramicidin channels and activate the channels in the absence of far-field tension.

Lundbaek and Andersen (1994) demonstrated that LPLs can increase the dimerization constant of membrane-bound gramicidin up to 500-fold (at the concentration of 2 μM). They found that the relative potency increases as a function of the size of the polar headgroup but does not depend on headgroup charge. It also depends on the channel length: as the channel length is decreased, the potency of the LPC increased.

Membrane curvature is extensively employed for explanation of mechanical membrane transformations in the process of membrane fusion, fission, and poration (cf. Markin and Albanesi, 2002; Tamm *et al*., 2003). The key idea is that bending energy per unit area of a monolayer is determined by the difference between the actual geometric curvature of the monolayer C, and its spontaneous curvature C_0 as

$$E_{\text{curvature}} = \frac{1}{2}\kappa_C(C - C_0)^2, \tag{41}$$

where κ_C is the bending modulus or curvature elasticity. In the region of hydrophobic mismatch, where deformation occurs, this quantity should be compared with the energy of the initial, planar monolayer so that the elastic energy change will be:

$$\Delta E_{\text{curvature}} = \frac{1}{2}\kappa_C (C - C_0)^2 - \frac{1}{2}\kappa_C C_0^2 = -\kappa_C C C_0 + \frac{1}{2}\kappa_C C^2 \qquad (42)$$

The mean geometrical curvature of the monolayers near a gramicidin channel is determined by the difference between monolayer hydrophobic thickness and the length of gA monomers. As a first approximation, the mean curvature can be presented as $C = \alpha(h_0 - l_g)$. Spontaneous curvature is created by the lysolipids and should be proportional to their concentration, $C_0 = \beta c_{\text{LPL}}$. The proportionality coefficient β can be positive, as for lysolipids (positive spontaneous curvature), or negative for other amphipaths.

The change of elastic energy of each monolayer (42) near the channel gives the contribution to Gibbs free energy of transition between closed and open states:

$$\Delta G = A_{\text{rim}}\kappa_C[\alpha^2(h_0 - l_g)^2 - 2\alpha\beta(h_0 - l_g)c_{\text{LPL}}] - G_{\text{ass}}, \qquad (43)$$

where A_{rim} is the area of the distorted lipid rim around gramicidin. According to Eq. (38), the number of dimers is given by

$$N_d = K_* N_{\text{tot}}^2 \exp\left(\frac{G_{\text{ass}}}{kT}\right) \exp\left\{\frac{A_{\text{rim}}\alpha^2\kappa_C\, h_0^2}{kT}\left[\frac{2\beta\, c_{\text{LPL}}}{\alpha h_0}\left(1 - \frac{l_g}{h_0}\right) - \left(1 - \frac{l_g}{h_0}\right)^2\right]\right\} \qquad (44)$$

We shall define the characteristic amount of dimers

$$N_d^0 = K_* N_{\text{tot}}^2 \exp\left[\frac{G_{\text{ass}} - A_{\text{rim}}\alpha^2\kappa_C(h_0 - l_g)^2}{kT}\right] \qquad (45)$$

that can be formed in the absence of lysolipids ($c_{\text{LPL}} = 0$) and introduce the degree of activation of channels by lysolipids:

$$q_{\text{act}} = \frac{N_d}{N_d^0} = \exp\left[\frac{2A_{\text{rim}}\alpha\beta\kappa_C\, h_0 c_{\text{LPL}}}{kT}\left(1 - \frac{l_g}{h_0}\right)\right] \equiv \exp\left[\frac{c_{\text{LPL}}}{c_{\text{LPL}}^0}\left(1 - \frac{l_g}{h_0}\right)\right] \qquad (46)$$

This equation introduces a characteristic concentration of lysolipids

$$c_{\text{LPL}}^0 = \frac{kT}{2A_{\text{rim}}\alpha\beta\kappa_C\, h_0 c_{\text{LPL}}} \qquad (47)$$

that determines the potency of the given type of LPL to activate the channel: the lower c_{LPL}^0 the higher is its potency. Lundbaek and Andersen (1994) observed that LPI and LPC are the most potent activators; at concentration of 2 μM they increased the number of open channels 630- and 450-fold, respectively, while LPE and LPS at the same concentration produce 80- and

40-fold increase. This is related to the shape of lysolipid molecules: The shape is conical and the angle of this cone is determined by the size of their polar headgroups which go along with this series. The size of the headgroups is determined not only by the atoms constituting the polar heads but the hydration of these heads. PC headgroups are much more hydrated than PE and PS headgroups. So the shape of LPL molecule accounts for the potency of different LPLs.

The reason we call q_{act} the degree of activation rather than open probability is that its value can exceed 1. Figure 13 presents function (46) for three different values of monolayer thickness. In thick membranes ($h_0 > l_g$) lysolipids activate channels even without membrane tension and q_{act} goes up. In thin membranes ($h_0 < l_g$) lysolipids inactivate channels and q_{act} goes down, and if the length of the gramicidin monomer coincides with the hydrophobic thickness of the monolayer there is no effect of LPL: q_{act} remains constant and equal to 1.

B. Other Parameters Regulating Switch Between Stretch-Activation and Inactivation Modes

The change of polarity of MS channels was described above in the example of gramicidin that does not preexist as a channel but rather forms

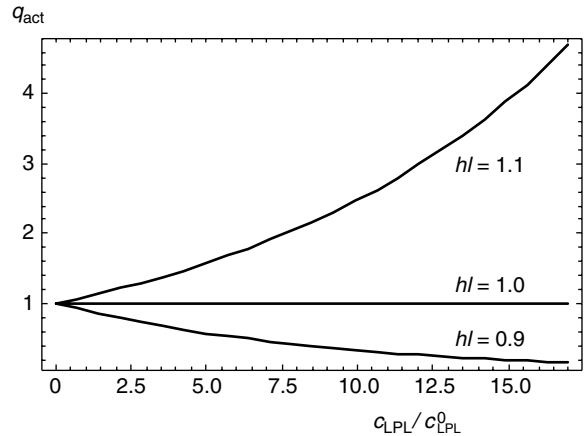

FIGURE 13 The degree of activation of gramicidin channels by LPLs. The curves are plotted according to Eq. (46). Channels are activated in thick membranes ($h_0 > l_g$) and inactivated in thin membranes ($h_0 < l_g$). The border line ($h_0 = l_g$) goes horizontally showing no effect in this case.

in process of mechanotransduction. But this phenomenon can also be observed in the preexisting channels where activation can be regulated by additional allosteric factors such as membrane potential. A well-known example is *Shaker*-IR, a voltage-gated K^+ channel. It can exhibit a rich behavior including transition from stretch-activation to stretch-inactivation depending on the value of the membrane potential (Gu *et al.*, 2001). The mechanism of this phenomenon is not known and Gu *et al.* (2001) discussed a multistate scheme where some states with different time scale can play decisive MS role.

Stretch-activation occurs in the channels that have rather low p_{open} at rest and stretch-inactivation at high p_{open}. This was demonstrated above with gramicidin channel. In *Shaker*, where electrical potential causes a shift of open probability, stretch tends to open closed channels and close open channels suggesting that an intermediate sate has significantly different geometry than the end states (Tabarean and Morris, 2002). The shift from SAC to SIC behavior has been shown in 2P K^+ channels (Honore *et al.*, 2006) and in MS channels from dystrophic muscle compared to normal muscle (Franco-Obregon and Lansman, 1994). However, it has been shown that SIC behavior can be produced by SACs that are under tension at rest (Honore *et al.*, 2006). Patches can be stressed by the cytoskeleton pulling the membrane toward the tip. Then suction can flatten the membrane reducing tension and closing the channels—SIC behavior. Thus, the difference between the dystrophic and normal muscle behavior may represent differences in cytoskeletal structure rather than channel structure (Suchyna and Sachs, 2007).

VI. THERMODYNAMIC APPROACH AND DETAILED MECHANICAL MODELS OF MS CHANNELS

When describing the mechanosensitivity phenomenon, we use the general thermodynamic approach which is free of specific model assumptions. The model-free thermodynamic approach is a powerful method permitting to establish the relationship between generalized forces and reactions of the system. A disadvantage is that it does not consider how mechanical forces gate the channel and leaves apart all parameters and specific properties of real systems. These properties can be found only in experimental studies and accounted for by mechanical models that need to include mechanics of the patch itself (Chiang *et al.*, 2004; Suchyna and Sachs, 2004; Honore *et al.*, 2006), and to include the heterogeneous distribution of mechanical stresses between the bilayer and the cytoskeleton.

Hamill and Martinac (2001) provided a list of specific models used by different authors to describe the behavior of MS channels, focusing on MscL. The first in this list is the multimerization model. It considered the tension-sensitive recruitment of MscL monomers into a multimeric pore. The recruitment occurs because the energy of the complex under tension is lower than the energy of separated monomers. In the thermodynamic approach, the additional energy (that can be either positive or negative) of the complex was associated with interaction energy at the border between the channel complex and surrounding lipid. As is customary in two-dimensional (2D) thermodynamics, this energy was described as a line tension. If the line tension decreases with area tension, then it favors formation (opening) of the channel, which will be stretch-activated. The multimerization model probably does not apply to MscL. One serious objection is the very rapid opening transition (i.e., $<$0.2 ms) (Hamill and Martinac, 2001) that would be difficult for monomer diffusion in a viscous membrane.

The second model of MscL is for an open channel with membrane-spanning α-helices normal to the membrane and forming a pore $\sim$4 nm in diameter. In this model, the channel must undergo a large conformational change where the close-packed membrane-spanning helices of the closed channel need to shift radially to open the pore to the observed 3.6 nm at the periplasmic end of the channel (Bass *et al.*, 2002). That would account for the large slope sensitivity of the channel corresponding to $\Delta A \sim 6$ nm^2. This was the model with expanding in-plane area that we discussed in this chapter.

The third model is an electromechanical coupling model that employs the idea of swinging gates. Gu *et al.* (1998) proposed that the pore region of MscL is present in the closed channel conformation and that the flexible N-terminus of the five subunits interact electrostatically to close and open the channel. Membrane tension would drive these five swinging gates to the open position. The model specifies the pivot point and the swing of the gates. The swinging gates driven by membrane tension put this model into the class with expanding area. This model probably does not apply to MscL since it predicts too small an energy difference between closed and open states (2 kT against actual 15 kT), and suffers some other limitations (Hamill and Martinac, 2001).

The fourth item is a five-state kinetic model of MscL (Sukharev *et al.*, 1999). It is based on the presence of multiple conducting states. The physical model uses the expanding area as described above, but is really a kinetic model, not a molecular one. However, the analysis does suggest that there is only one tension-sensitive transition and that the closed state is more compliant than the conducting states.

A. Detailed Mechanical Models

Opening and closing of MS channels were also addressed with detailed mechanical models by different authors. A specific model approach was presented by Wiggins and Phillips (2004, 2005) who concentrated on the deformation of the lipid bilayer surrounding the MS channel. They found that the bilayer deformation free energy can be of the same order as the free energy differences between conformational states of the MscL channel and hence bilayer deformation can play an important role in determining the protein conformation. They applied the classical model of membrane elastic deformation by Canham (1970) and Helfrich and Jakobsson (1990) with the model of Huang (1986a,b) for the deformation energy induced by inclusions. They estimated different contributions to the total free energy, for example: area deformation $\sim 10\ kT$, Gaussian curvature $\sim 1\ kT$, spontaneous curvature $\sim 10\ kT$, bilayer interface $\sim 10\ kT$, midplane deformation $< 1\ kT$, thickness deformation $\sim 10\ kT$. These order of magnitude estimates give the idea of the possible energies involved in mechanosensitivity. Changing of these energies by various stresses determines the open probability and the rate of transition.

In this connection, hydrophobic mismatch between membrane proteins and surrounding lipids attracts significant interest of many authors. The thickness of this hydrophobic portion of the protein is particularly important. Exposing hydrophobic fatty acyl chains or peptide residues to water is energetically costly, and hydrophobic regions of the peptide should match the hydrophobic thickness of the bilayer. Theoretical models assumed that lipid molecules in the vicinity of proteins deform their tails to adjust to the hydrophobic length of the protein. This involves a number of contributions to the mismatch energy (O'Keeffe *et al.*, 2000): (i) loss of conformational entropy of the chains imposed by the presence of the rigid protein wall, (ii) bilayer compression/expansion energy due to changes in the membrane thickness, (iii) surface energy changes due to changes in area of the bilayer–water interface, and (iv) splay energy due to changes in the cross-sectional area available to the chains along their length, resulting from curvature of the monolayer surface near the protein.

A number of theoretical models have been proposed to estimate these terms (Fattal and Benshaul, 1993; Nielsen *et al.*, 1998a,b). Elmore and Dougherty (2001) published molecular dynamic simulation of this phenomenon. Experimentally, this energy was evaluated by Trp fluorescence spectroscopy (O'Keeffe *et al.*, 2000; Powl *et al.*, 2003, 2005). Wiggins and Phillips used these data to calculate the line tension at the protein–lipid border. As in Markin and Sachs (2004), they assumed that the acyl-chain length

of 16 corresponds to zero mismatch, implying that the thickness of the closed state equals the equilibrium thickness of the bilayer. They presented a series of data of line tensions of different proteins together with theoretical estimates. These data range from 0 to 1.5 kT/nm, which translate to 0–6 pN. Markin and Sachs (2004) using data of Perozo *et al.* (2002) estimated a line tension of 10 and 25 pN.

An interesting estimate of the variation of line tension is offered (Hamill and Martinac, 2002) when membrane tension is applied to the MS channel. MscL opens at membrane tension close to the lytic tension. At the lytic tension, the lipid bilayer thins by 2–4%, or 0.07–0.14 nm. Taking the diameter of MscL equal to 5 nm and hydrophobic energy 17 mJ/m^2, they estimated 2.7–4.8 $\times$ 10^{-20} J or 7–18 kT for the hydrophobic mismatch energy at the midpoint of the gating tension. This means that additional contribution to the line tension appears at this moment and it is 1.2–2.4 pN.

VII. CONCLUSIONS

The phenomenon of mechanosensitivity was described in terms of basic membrane forces: membrane tension, line tension, and membrane torque. Their geometrical counterparts are in-plane area, length of the border between the channel and lipid and the channel shape. A separate position is occupied by the length of the channel. The hydrophobic mismatch between channel and lipid bilayer actually generates a force normal to the bilayer that pulls the parts of the channel into membrane or pushes them out. The resulting effect was parameterized by the line tension representing the energy of mismatch. This approach provides a simple and efficient method of analysis of MS channels, for example how the gating of MS channels changes with bilayer thickness and stiffness. The effects were mediated through the line tension and this parameter was found using existing experimental data.

If the MS channel changes its shape in transition, then its gating is influenced by membrane torque which is created by global and/or local membrane bending. Amphipaths can open or close channels without the application of far-field tension. This explains numerous observations of action of lysolipids and other amphiphiles on channel gating.

The thermodynamic approach permits analysis of both SAC and SIC. The model gramicidin channel does not preexist in the closed state but rather forms the open state in the MS transition. Depending on the bilayer thickness, gramicidin can be either a SAC or SIC. This result demonstrates the predictive power of this approach, and it explains how the switch between SAC and SIC activity can occur without changing bilayer composition.

It is important to be able to distinguish the mechanism of mechanosensitivity in a particular case. One tool is to analyze the relationship of open probability to membrane tension or other parameters. In the simplest case, it is a Boltzmann function where the free energy depends linearly on membrane tension. However, this dependence may be nonlinear as was shown for gramicidin.

The discussion above focuses on the equilibrium distribution of channels between open and closed states. The kinetics stand apart. For example, in the process of opening and closing, the channel goes through transition states that can have different sizes and/or shapes. Conti *et al.* (1984) studied how gating of the Na^+ channel in squid axon depended on hydrostatic pressure, and found that the rate limiting activation step had a large positive activation volume. Of course, this is a three-dimensional volume increase, but it will translate into 2D areas and shapes, as in the case of the voltage-sensitive channels (Laitko and Morris, 2004). Furthermore, the net free energy change will depend on the relative compressibility of the components (water, lipids, and proteins). The rate constants may depend on membrane tension or membrane torque, *even if the equilibrium open probabilities are not mechanosensitive*! The thermodynamic approach can be effectively used to analyze the mechanism of action of pharmacological agents—mechanopharmacology (Suchyna *et al.*, 2004a). For example, one of popular inhibitors of MS channels is Gd^{+3}, and as shown in the analysis of membrane thickness on MscL gating, if Gd^{+3} acts by changing lipid stiffness, it should produce a correlated change in the midpoint and the slope of the gating curve.

References

Akinlaja, J., and Sachs, F. (1998). The breakdown of cell membranes by electrical and mechanical stress. *Biophys. J.* **75,** 247–254.

Andersen, O. S., Saberwal, G., Greathouse, D. V., and Koeppe, R. E. (1996). Gramicidin channels—a solvable membrane "protein" folding problem. *Indian J. Biochem. Biophys.* **33,** 331–342.

Anishkin, A., and Sukharev, S. (2004). Mechanosensitive channels: What can we learn from 'simple' model systems? *Trends Neurosci.* **27,** 345–351.

Bass, R. B., Strop, P., Barclay, M., and Rees, D. C. (2002). Crystal structure of *Escherichia coli* MscS, a voltage-modulated and mechanosensitive channel. *Science* **298,** 1582–1587.

Betanzos, M., Chiang, C. S., Guy, H. R., and Sukharev, S. (2002). A large iris-like expansion of a mechanosensitive channel protein induced by membrane tension. *Nat. Struct. Biol.* **9,** 704–710.

Bowman, C. B., and Lohr, J. W. (1996a). Curvature sensitive mechanosensitive ion channels and osmotically evoked movements of the patch membrane. *Biophys. J.* **70,** A365.

Bowman, C. L., and Lohr, J. W. (1996b). Mechanotransducing ion channels in C6 glioma cells. *Glia* **18,** 161–176.

Calabrese, B., Tabarean, I. V., Juranka, P., and Morris, C. E. (2002). Mechanosensitivity of N-type calcium channel currents. *Biophys. J.* **83,** 2560–2574.

Canham, P. B. (1970). The minimum energy of bending as a possible explanation of the biconcave shape of the human red blood cell. *J. Theor. Biol.* **26,** 61–81.

Chiang, C. S., Anishkin, A., and Sukharev, S. (2004). Gating of the large mechanosensitive channel *in situ*: Estimation of the spatial scale of the transition from channel population responses. *Biophys. J.* **86,** 2846–2861.

Conti, F., Inoue, I., Kukita, F., and Stuhmer, W. (1984). Pressure-dependence of sodium gating currents in the squid giant-axon. *Eur. Biophys. J.* **11,** 137–147.

Elmore, D. E., and Dougherty, D. A. (2001). Molecular dynamics simulations of wild-type and mutant forms of the Mycobacterium tuberculosis MscL channel. *Biophys. J.* **81,** 1345–1359.

Evans, E., Heinrich, V., Ludwig, F., and Rawicz, W. (2003). Dynamic tension spectroscopy and strength of biomembranes. *Biophys. J.* **85,** 2342–2350.

Fattal, D. R., and Benshaul, A. (1993). A molecular-model for lipid-protein interaction in membranes—the role of hydrophobic mismatch. *Biophys. J.* **65,** 1795–1809.

Franco-Obregon, A., Jr., and Lansman, J. B. (1994). Mechanosensitive ion channels in skeletal muscle from normal and dystrophic mice. *J. Physiol.* **481,** 299–309.

Garcia-Anoveros, J., and Corey, D. P. (1996). Mechanosensation: Touch at the molecular level. *Curr. Biol.* **6,** 541–543.

Goulian, M., Feygenson, D., Mesquita, O. N., Moses, E., Nielsen, C., Andersen, O. S., and Libchaber, A. (1997). The effect of membrane tension on gramicidin A channel kinetics. *Biophys. J.* **72,** TU309.

Gradmann, D., and Boyd, C. M. (2005). Fast, triangular voltage clamp for recording and kinetic analysis of an ion transporter expressed in *Xenopus* oocytes. *Biophys. J.* **89,** 734–744.

Gu, C. X., Juranka, P. F., and Morris, C. E. (2001). Stretch-activation and stretch-inactivation of Shaker-IR, a voltage- gated K+ channel. *Biophys. J.* **80,** 2678–2693.

Gu, L., Liu, W., and Martinac, B. (1998). Electromechanical coupling model of gating the large mechanosensitive ion channel (MscL) of *Escherichia coli* by mechanical force. *Biophys. J.* **74,** 2889–2902.

Hackney, C. M., and Furness, D. N. (1995). Mechanotransduction in vertebrate hair cells: Structure and function of the stereociliary bundle (Review). *Am. J. Physiol.* **268,** C1–C13.

Hamill, O. P., and Martinac, B. (2001). Molecular basis of mechanotransduction in living cells. *Physiol. Rev.* **81,** 685–740.

Hase, C. C., Le Dain, A. C., and Martinac, B. (1995). Purification and functional reconstitution of the recombinant large mechanosensitive ion channel (MscL) of *Escherichia coli*. *J. Biol. Chem.* **270,** 18329–18334.

Helfrich, P., and Jakobsson, E. (1990). Calculations of deformation energies and conformations in lipid membranes containing gramicidin channels. *Biophys. J.* **57,** 1075–1084.

Hladky, S. B., and Haydon, D. A. (1972). Ion transfer across lipid membranes in the presence of gramicidin A. I. Studies of the unit conductance channel. *Biochim. Biophys. Acta* **274,** 294–312.

Honore, E., and Patel, A. A. (2004). Potassium-selective cardiac mechano-sensitive ion channels. *In* "Cardiac Mechano-Electric Feedback and Arrhythmias: From Pipette to Patient" (P. Kohl, M. R. Franz, and F. Sachs, eds.). Elsevier, Philadelphia.

Honore, E., Patel, A. J., Chemin, J., Suchyna, T., and Sachs, F. (2006). Desensitization of mechano-gated K2P channels. *Proc. Natl. Acad. Sci. USA* **103,** 6859–6864.

Huang, H. W. (1986a). Deformation free energy of bilayer membrane and its effect on gramicidin channel lifetime. *Biophys. J.* **50,** 1061–1070.

Huang, H. W. (1986b). Effect of membrane thickness on gramicidin channel lifetime. *Biophys. J.* **49,** A148.

Hwang, T. C., Koeppe, R. E., and Andersen, O. S. (2003). Genistein can modulate channel function by a phosphorylation-independent mechanism: Importance of hydrophobic mismatch and bilayer mechanics. *Biochemistry* **42,** 13646–13658.

Iscla, I., Levin, G., Wray, R., Reynolds, R., and Blount, P. (2004). Defining the physical gate of a mechanosensitive channel, MscL, by engineering metal-binding sites. *Biophys. J.* **87,** 3172–3180.

Jutabha, P., Kanai, Y., Hosoyamada, M., Chairoungdua, A., Kim, D. K., Iribe, Y., Babu, E., Kim, J. Y., Anzai, N., Chatsudthipong, V., and Endou, H. (2003). Identification of a novel voltage-driven organic anion transporter present at apical membrane of renal proximal tubule. *J. Biol. Chem.* **278,** 27930–27938.

Kim, C. (2004). Transient receptor potential ion channels and animal sensation: Lessons from Drosophila functional research. *J. Biochem. Mol. Biol.* **37,** 114–121.

Kloda, A., and Martinac, B. (2001). Molecular identification of a mechanosensitive channel in archaea. *Biophys. J.* **80,** 229–240.

Laitko, U., and Morris, C. E. (2004). Membrane tension accelerates rate-limiting voltage-dependent activation and slow inactivation steps in a shaker channel. *J. Gen. Physiol.* **123,** 135–154.

Lee, K. J. B. (2006). Energetics of rotational gating mechanisms of an ion channel induced by membrane deformation. *Phys. Rev. E. Stat. Nonlin. Soft. Matter Phys.* **73,** 021909.

Lin, S. Y., Holt, J. R., Vollrath, M. A., Garcia-Anoveros, J., Geleoc, G., Kwan, K., Hoffman, M. P., Zhang, D. S., and Corey, D. P. (2005). TRPA1 is a candidate for the mechanosensitive transduction channel of vertebrate hair cells. *Biophys. J.* **88,** 287A–288A.

Lundbaek, J. A., and Andersen, O. S. (1994). Lysophospholipids modulate channel function by altering the mechanical properties of lipid bilayers. *J. Gen. Physiol.* **104,** 645–673.

Lundbaek, J. A., and Andersen, O. S. (1999). Spring constants for channel-induced lipid bilayer deformations. Estimates using gramicidin channels. *Biophys. J.* **76,** 889–895.

Lundbaek, J. A., Maer, A. M., and Andersen, O. S. (1997). Lipid bilayer electrostatic energy, curvature stress, and assembly of gramicidin channels. *Biochemistry* **36,** 5695–5701.

Maingret, F., Fosset, M., Lesage, F., Lazdunski, M., and Honore, E. (1999). TRAAK is a mammalian neuronal mechano-gated K^+ channel. *J. Biol. Chem.* **274,** 1381–1387.

Maingret, F., Patel, A. J., Lesage, F., Lazdunski, M., and Honore, E. (2000). Lysophospholipids open the two-pore domain mechano-gated K(+) channels TREK-1 and TRAAK. *J. Biol. Chem.* **275,** 10128–10133.

Maingret, F., Honore, E., Lazdunski, M., and Patel, A. J. (2002). Molecular basis of the voltage-dependent gating of TREK-1, a mechano-sensitive K(+) channel. *Biochem. Biophys. Res. Commun.* **292,** 339–346.

Markin, V. S., and Albanesi, J. P. (2002). Membrane fusion: Stalk model revisited. *Biophys. J.* **82,** 693–712.

Markin, V. S., and Martinac, B. (1991). Mechanosensitive ion channels as reporters of bilayer expansion. A theoretical model. *Biophys. J.* **60,** 1120–1127.

Markin, V. S., and Sachs, F. (2004). Thermodynamics of mechanosensitivity. *Phys. Biol.* **1,** 110–124.

Maroto, R., Raso, A., Wood, T. G., Kurosky, A., Martinac, B., and Hamill, O. P. (2005). TRPC1 forms the stretch-activated cation channel in vertebrate cells. *Nat. Cell Biol.* **7,** 179–185. Jan 23, 2005 (epub).

Martinac, B. (2001). Mechanosensitive channels in prokaryotes. *Cell. Physiol. Biochem.* **11,** 61–76.

Martinac, B., and Hamill, O. P. (2002). Gramicidin A channels switch between stretch activation and stretch inactivation depending on bilayer thickness. *Proc. Natl. Acad. Sci. USA* **99,** 4308–4312.

Martinac, B., Adler, J., and Kung, C. (1990). Mechanosensitive ion channels of *E. coli* activated by amphipaths. *Nature* **348,** 261–263.

Moe, P., and Blount, P. (2005). Assessment of potential stimuli for mechano-dependent gating of MscL: Effects of pressure, tension, and lipid headgroups. *Biochemistry* **44,** 12239–12244.

Morris, C. E. (2004). Stretch effects on voltage-gated channels in cardiac cells. *In* "Cardiac Mechano-Electric Feedback and Arrhythmias: From Pipette to Patient" (P. Kohl, F. Sachs, and M. R. Franz, eds.). Elsevier, Philadelphia.

Morris, C. E., and Sigurdson, W. J. (1989). Stretch-inactivated ion channels coexist with stretch-activated ion channels. *Science* **243,** 807–809.

Nielsen, C., Goulian, M., and Andersen, O. S. (1998a). Energetics of inclusion-induced bilayer deformations. *Biophys. J.* **74,** 1966–1983.

Nielsen, C., Goulian, M., and Anderson, O. S. (1998b). Energetics of membrane deformation in systems with non-zero monolayer curvature. *Biophys. J.* **74,** A309.

O'Keeffe, A. H., East, J. M., and Lee, A. G. (2000). Selectivity in lipid binding to the bacterial outer membrane protein OmpF. *Biophys. J.* **79,** 2066–2074.

Opsahl, L. R., and Webb, W. W. (1994). Lipid-glass adhesion in giga-sealed patch-clamped membranes. *Biophys. J.* **66,** 75–79.

Patel, A. J., Honore, E., Lesage, F., Fink, M., Romey, G., and Lazdunski, M. (1999). Inhalational anesthetics activate two-pore-domain background K+ channels. *Nat. Neurosci.* **2,** 422–426.

Patel, A. J., Lazdunski, M., and Honore, E. (2001). Lipid and mechano-gated 2P domain K(+) channels. *Curr. Opin. Cell Biol.* **13,** 422–428.

Perozo, E., and Rees, D. C. (2003). Structure and mechanism in prokaryotic mechanosensitive channels. *Curr. Opin. Struct. Biol.* **13,** 432–442.

Perozo, E., Cortes, D. M., Sompornpisut, P., Kloda, A., and Martinac, B. (2002). Open channel structure of MscL and the gating mechanism of mechanosensitive channels. *Nature* **418,** 942–948.

Petrov, A. G. (1999). "The Lyotropic State of Matter," 1st edn. Gordon and Breach Science Publishers, Amsterdam.

Petrov, A. G., and Usherwood, P. N. (1994). Mechanosensitivity of cell membranes. Ion channels, lipid matrix and cytoskeleton (Review) (95 refs). *Eur. Biophys. J.* **23,** 1–19.

Powl, A. M., East, J. M., and Lee, A. G. (2003). Lipid-protein interactions studied by introduction of a tryptophan residue: The mechanosensitive channel MscL. *Biochemistry* **42,** 14306–14317.

Powl, A. M., Carney, J., Marius, P., East, J. M., and Lee, A. G. (2005). Lipid interactions with bacterial channels: Fluorescence studies. *Biochem. Soc. Trans.* **33,** 905–909.

Sachs, F., and Lecar, H. (1991). Stochastic models for mechanical transduction (letter). *Biophys. J.* **59,** 1143–1145.

Sachs, F., and Morris, C. E. (1998). Mechanosensitive ion channels in non specialized cells. *In* "Reviews of Physiology and Biochemistry and Pharmacology" (M. P. Blaustein, R. Greger, H. Grunicke, R. Jahn, L. M. Mendell, A. Miyajima, D. Pette, G. Schultz, and M. Schweiger, eds.), pp. 1–78. Springer, Berlin.

Sokabe, M., Sachs, F., and Jing, Z. (1991). Quantitative video microscopy of patch clamped membranes—stress, strain, capacitance and stretch channel activation. *Biophys. J.* **59,** 722–728.

Suchyna, T., and Sachs, F. (2004). Dynamic regulation of mechanosensitive channels: Capacitance used to monitor patch tension in real time. *Phys. Biol.* **1,** 1–18.

Suchyna, T., and Sachs, F. (2007). Mechanical and electrical properties of membranes from dystrophic and normal mouse muscle. *J. Physiol. (Lond).* (in press).

Suchyna, T., Tape, S. E., Koeppe, R. E., Andersen, O. S., Sachs, F., and Gottlieb, P. (2004a). Non chiral effects of a peptide inhibitor of mechanosensitive channels: Evidence for a bilayer-dependent mechanism. *Nature* **430,** 235–240.

Suchyna, T. M., Tape, S. E., Koeppe, R. E., Andersen, O. S., Sachs, F., and Gottlieb, P. A. (2004b). Bilayer-dependent inhibition of mechanosensitive channels by neuroactive peptide enantiomers. *Nature* **430,** 235–240.

Sukharev, S., and Anishkin, A. (2004). Water dynamics and dewetting transitions in the small mechanosensitive channel MscS. *Biophys. J.* **86,** 2883–2895.

Sukharev, S., Sigurdson, W., Kung, C., and Sachs, F. (1999). Energetic and spatial parameters for gating of the bacterial large conductance mechanosensitive channel, MscL. *J. Gen. Physiol.* **113,** 525–539.

Sukharev, S. I., and Markin, V. S. (2001). Kinetic model of the bacterial large conductance mechanosensitive channel. *Biol. Membr.* **18,** 440–445.

Tabarean, I. V., and Morris, C. E. (2002). Membrane stretch accelerates activation and slow inactivation in Shaker channels with S3-S4 linker deletions. *Biophys. J.* **82,** 2982–2994.

Tamm, L. K., Crane, J., and Kiessling, V. (2003). Membrane fusion: A structural perspective on the interplay of lipids and proteins. *Curr. Opin. Struct. Biol.* **13,** 453–466.

Walker, R. G. (2000). A Drosophila mechanosensory transduction channel (Article). The Drosophila genome. *Science* **287,** 2229–2234.

Wiggins, P., and Phillips, R. (2004). Analytic models for mechanotransduction: Gating a mechanosensitive channel. *PNAS* **101,** 4071–4076.

Wiggins, P., and Phillips, R. (2005). Membrane-protein interactions in mechanosensitive channels. *Biophys. J.* **88,** 880–902.